Early detection of ocean acidification effects on marine calcification

Tatjana Ilyina,[1] Richard E. Zeebe,[1] Ernst Maier-Reimer,[2] and Christoph Heinze[3]

[1] Ocean acidification is likely to impact calcification rates in many pelagic organisms, which may in turn cause significant changes in marine ecosystem structure. We examine effects of changes in marine $CaCO_3$ production on total alkalinity (TA) in the ocean using the global biogeochemical ocean model HAMOCC. We test a variety of future calcification scenarios because experimental studies with different organisms have revealed a wide range of calcification sensitivities to $CaCO_3$ saturation state. The model integrations start at a preindustrial steady state in the year 1800 and run until the year 2300 forced with anthropogenic CO_2 emissions. Calculated trends in TA are evaluated taking into account the natural variability in ocean carbonate chemistry, as derived from repeat hydrographic transects. We conclude that the data currently available does not allow discerning significant trends in TA due to changes in pelagic calcification caused by ocean acidification. Given different calcification scenarios, our model calculations indicate that the TA increase over time will start being detectable by the year 2040, increasing by $5-30$ μmol kg^{-1} compared to the present-day values. In a scenario of extreme reductions in calcification, large TA changes relative to preindustrial conditions would have occurred at present, which we consider very unlikely. However, the time interval of reliable TA observations is too short to disregard this scenario. The largest increase in surface ocean TA is predicted for the tropical and subtropical regions. In order to monitor and quantify possible early signs of acidification effects, we suggest to specifically target those regions during future ocean chemistry surveys.

Citation: Ilyina, T., R. E. Zeebe, E. Maier-Reimer, and C. Heinze (2009), Early detection of ocean acidification effects on marine calcification, *Global Biogeochem. Cycles*, *23*, GB1008, doi:10.1029/2008GB003278.

1. Introduction

[2] The ocean is taking up a large fraction of the carbon dioxide (CO_2) that is released to the atmosphere by mankind. As CO_2 invades the ocean, the seawater becomes less alkaline and the pH drops, a process termed ocean acidification. Because of the oceanic uptake of CO_2, the marine carbonate chemistry is currently perturbed and will be perturbed even more significantly in the future [e.g., *Wolf-Gladrow et al.*, 1999; *Kleypas et al.*, 1999; *Feely et al.*, 2008]. For example, the pH of seawater has decreased by 0.1 units during the 20th century [*Intergovernmental Panel on Climate Change*, 2007] and is expected to fall by 0.7 units in less than 500 years, which is unprecedented in Earth's history over the past 300 million years, regarding magnitude and rate of pH change [*Caldeira and Wickett*, 2003]. As a result, surface ocean $CaCO_3$ saturation states are projected to decrease by about 40% until the year 2100 [e.g., *Zeebe and Wolf-Gladrow*, 2001; *Raven et al.*, 2005; *Kleypas et al.*, 2006].

[3] Diminished $CaCO_3$ saturation state leads to a reduction of calcification rates at the organism level in many species of the most important calcifying groups in the ocean, i.e., in coccolithophorids, foraminifera, and corals by up to 83% [e.g., *Riebesell et al.*, 2000; *Bijma et al.*, 1999; *Leclercq et al.*, 2000; *Langdon and Atkinson*, 2005; *Gazeau et al.*, 2007]. On the other hand, while $CaCO_3$ production may be impaired in most species at the organism level, certain calcifying groups such as coccolithophores may benefit from a stronger stratification in a warmer future [*Nanninga and Tyrrell*, 1996; *Tyrrell and Merico*, 2004]. It is also unknown whether calcifiers can adapt to decreasing saturation state. Recent laboratory experiments with two coccolithophorid species [*Langer et al.*, 2006] showed a nonlinear relationship between changes in calcification and increasing CO_2 concentration. The study also provides evidence for little or no change in calcification at elevated CO_2 concentration. In summary, calcifying organisms show a wide range of sensitivities of calcification to saturation state. The response to ocean acidification in different groups and even species is therefore likely to be inhomogeneous and ecosystem response on a global scale is unknown.

[4] Changes in marine calcification due to ocean acidification can be detected and quantified via their effect on the ocean chemistry: Any shift in the vertical carbonate or

[1]Department of Oceanography, School of Ocean and Earth Science and Technology, University of Hawaii, Honolulu, Hawaii, USA.
[2]Max Planck Institute for Meteorology, Hamburg, Germany.
[3]Geophysical Institute and Bjerknes Centre for Climate Research, University of Bergen, Bergen, Norway.

organic carbon flux due to production and dissolution of $CaCO_3$ affects the vertical distribution of total alkalinity (henceforth TA). A global model can show where these changes in TA will likely occur and indicate the magnitude and relevant timescales. However, only the field data will tell whether those changes actually occur in nature.

[5] A few modeling studies on the effects of changing marine calcification on the global carbon cycle and on the long-term future of marine calcification have been conducted recently [*Gehlen et al.*, 2007; *Ridgwell et al.*, 2007; *Andersson et al.*, 2006; *Heinze*, 2004]. Data sets on ocean carbonate chemistry were obtained during various ocean-survey programs, for example WOCE and CLIVAR [*Key et al.*, 2004]. However, so far modeling efforts and ocean carbon chemistry observations have usually been considered separately.

[6] Our study combines ocean chemistry data and quantitative modeling using the global biogeochemical ocean model HAMOCC. By employing TA measurements from repeat hydrographic surveys and modeled alkalinity distributions, we develop a tool for early detection of ocean acidification effects on pelagic calcification. We employ a synthesis of modeling and ocean chemistry data in order to address the following question: Does ocean acidification lead to a decline in marine calcification on a global/ecosystem scale, and if so, what is the magnitude and timescale of the decline? This tool can be used to guide observational programs in the near future in order to identify target areas that are critical for determining the exact magnitude of acidification effects from field data.

2. Method Description

2.1. HAMOCC Model

[7] We use the global Hamburg ocean carbon cycle model HAMOCC designed for time-effective climate modeling studies [*Maier-Reimer*, 1993; *Archer et al.*, 1998; *Heinze and Maier-Reimer*, 1999]. The ecosystem cycles are based on nutrients, phytoplankton, zooplankton and detritus (NPZD type) [*Six and Maier-Reimer*, 1996; *Aumont et al.*, 2003]. Cycling of nitrate, phosphate and opal (co-limiting nutrients), as well as calcium carbonate, oxygen and oceanic carbon is included in the model. Processes like denitrification and N-fixation, formation of calcium carbonate and opaline shells are also considered. Nutrient uptake (input) and remineralization of organic matter (output) connects the global biogeochemical cycles and the trophic levels represented in the model. The ocean carbon cycle model advects chemical tracers using a steady flow field calculated by the Large-Scale Geostrophic Ocean General Circulation Model, tuned to represent the present-day ocean [*Maier-Reimer et al.*, 1993].

[8] The model has a realistic topography and a horizontal resolution of 3.5 by 3.5 degrees. In the vertical dimension, it has 22 layers of varying depth, i.e., 25 m at the ocean surface and up to 700 m in the deep-sea. At the seafloor, the model has 12 layers of bioturbated sediment with pore water geochemistry following *Heinze et al.* [2003]. The model also includes an atmospheric module, mixed zonally and with diffusive meridional transport of tracers.

[9] The total alkalinity for the seawater compounds represented in the model is described in accordance with the definition given by *Dickson* [1981]. Note, however, that contributions of, for example, S, Si, and P are not included in the model's total alkalinity description. Among the physical factors that control the alkalinity in the surface ocean (defined as the upper 100 m euphotic zone, corresponding to the upper two layers of the model) is the freshwater cycle, i.e., precipitation and evaporation, and mixing. The production and dissolution of calcium carbonate shells decreases and increases TA and total dissolved inorganic carbon (DIC) in a ratio 2:1. The production and remineralization of organic matter results in a decrease and increase of DIC, respectively. This process also slightly changes TA, mostly because of the uptake and release of nitrate. Although there are indications that river runoff may also increase TA [*Jones et al.*, 2003], it is constant in our simulations. In the deep ocean, alkalinity and DIC distributions are mostly a result of the large-scale ocean circulation and remineralization of carbonate and organic carbon, where the latter is calculated using the constant stoichiometric ratios N:P and C:P, respectively. Total dissolved inorganic carbon, total alkalinity, and atmospheric CO_2 are prognostic variables in the model.

[10] The model integrations start at a pre-industrial steady state in the year 1800 generated by a model spin-up of several thousand years and run until the year 2300. The model runs with a time step of 1 month forced by anthropogenic CO_2 emissions. Anthropogenic emissions used in the model combine historic emissions (G. Marland et al., 2003, Global, regional and national CO_2 emissions, in *Trends: A Compendium of Data on Global Change*, technical report, Carbon Dioxide Information Analysis Center, Oak Ridge National Laboratory, U.S. Department of Energy, Oak Ridge, Tennessee, available online at http://cdiac.esd.ornl.gov/trends/emis/tre_glob.html) for the period 1800–2000, and the IPCC emission scenario for 2001–2100 (based on the IS92a scenario), which includes (1) the very rapid economic growth, with the global population peaking around 2050 and decline thereafter and (2) the introduction of new effective technologies [*Intergovernmental Panel on Climate Change*, 2001]. Accordingly, CO_2 emissions reach their maximum in the mid-century and decline afterward (Figure 1). The ocean flow field was invariant during the model integration, neglecting possible climate feedbacks on ocean circulation. This allows detecting shifts in global ocean carbon chemistry caused by changes in the ocean carbon cycle.

2.2. Calcification Scenarios

[11] The global oceanic calcification is parameterized in the model as a function of the surface ocean carbonate ion concentration $[CO_3^{2-}]$, predicted from DIC and TA in the surface ocean. Export of calcite and opal particles are steered by the availability of dissolved Si. The biogenic $CaCO_3$ production (P_{CaCO3} expressed in units of mole C per unit area and unit time) is calculated as

$$P_{CaCO3} = a \cdot r \cdot \left(P_{orgC} - 0.5 \cdot P_{bioSi} \right) \qquad (1)$$
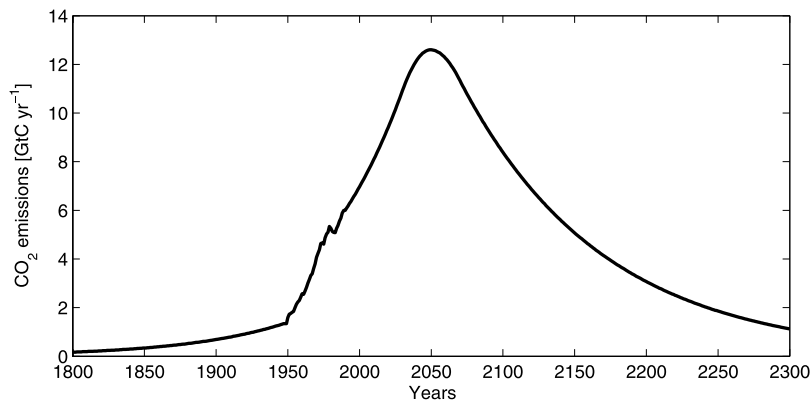
Figure 1. Anthropogenic CO_2 emissions (Gt C a^{-1}) for the period of 1800–2300 according to the emission scenario used in model calculations.

where P_{orgC} is the total organic primary production and P_{bioSi} is the total biogenic silica production expressed in units of mole C and Si, respectively, per unit time and unit area. The tunable parameter a is prescribed to 0.15 in this study. The rate coefficient r is calculated as a function of the $CaCO_3$ saturation state of seawater (Ω) which refers to calcite or aragonite and is defined as

$$\Omega = \frac{\left[Ca^{2+}\right] \times \left[CO_3^{2-}\right]}{K_{sp}^*} \qquad (2)$$

where $[Ca^{2+}]$ is the calcium ion concentration (constant at 10 mmol kg^{-1} in the model), $[CO_3^{2-}]$ is the carbonate ion concentration of seawater, and K_{sp}^* is the stoichiometric solubility product for $CaCO_3$ at in situ pressure.

[12] During the last few years it has been established that calcification in many species of the major $CaCO_3$ producing organisms in the ocean is susceptible to changes in the $CaCO_3$ saturation state of seawater. However, the response of calcifying organisms to changes in saturation state seen in experiments with, e.g., coccolithophores and foraminifera is inhomogeneous. Thus, it is difficult to prescribe a single scenario for changes in future calcification that will cover the complete community response. Therefore, we test different scenarios of calcification rate change as a function of the saturation state for calcite (Figure 2).

[13] Scenarios range from a linear decrease in calcification rate with $[CO_3^{2-}]$ concentration of up to 80% for a 40% reduction in calcite saturation state reported from ship board incubations of natural plankton assemblages [*Riebesell et al.*, 2000] to a parabolic decrease (moderate and extreme scenarios) as observed in corals [cf. *Langdon and Atkinson*, 2005; *Kleypas et al.*, 2006]. Recent laboratory experiments [*Langer et al.*, 2006] provide evidence for little or no changes in calcification of some species. Thus, we also run stabilization scenarios in which calcification rates decrease similar to the linear scenario but remain constant after a prescribed time interval. Two stabilization scenarios are tested. In the first scenario (stabilization$_{1/2}$), calcification rates stabilize after a 1/2 reduction in the saturation state with respect to the pre-industrial (initial) levels. In the second scenario (stabilization$_{2/3}$), stabilization begins after

calcite saturation state reaches 2/3 of the pre-industrial value. Note that critical reductions in calcite saturation state are attained at different model grid points at different times throughout the simulation period.

[14] The extreme, moderate, linear and stabilization scenarios are compared to a constant calcification run. In the constant scenario, the calcification rate was fixed at the pre-industrial level. The different dependencies of calcification rate on the saturation state are parameterized by the rate coefficient r included in the biogenic $CaCO_3$ production calculations (cf. equation (1); see Figure 2).

3. Alkalinity in the Modern Ocean

[15] We compare measured alkalinity distributions in the global surface ocean to modeled distributions in order to test the model's performance. Total alkalinity from the Global
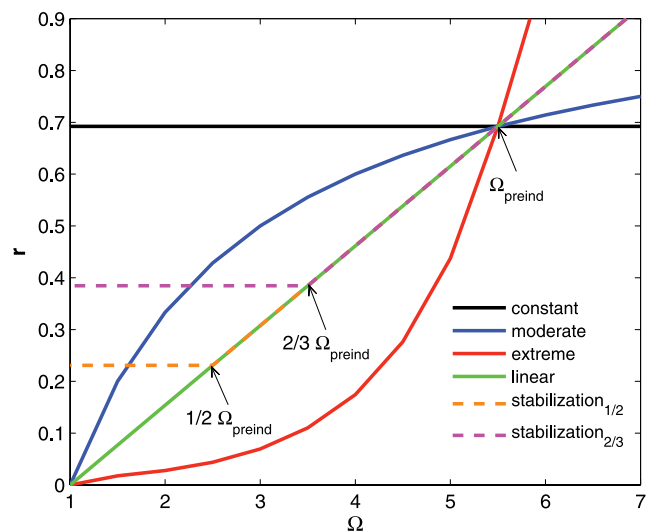
Figure 2. Various model scenarios of the response of calcifying organisms to changes in saturation state (Ω, equation (2)). Calcification rate dependency on Ω is parameterized by the rate coefficient r. Arrows point to Ω values reduced to 1/2 and 2/3 with respect to given preindustrial Ω.
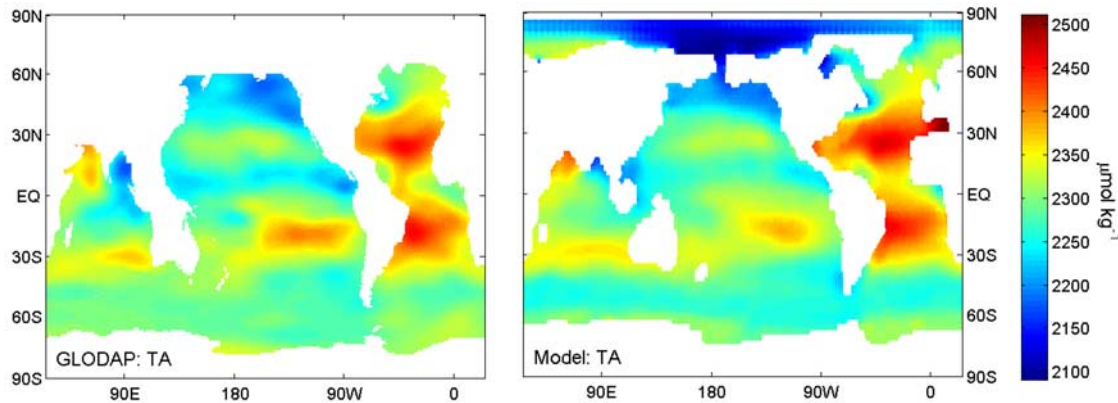
Figure 3. Total alkalinity (μmol kg^{-1}) from Global Ocean Data Analysis Project (GLODAP) (left) and calculated by the model (right; constant scenario, mean of 1980–1995).

Ocean Data Analysis Project (GLODAP) data set calculated from diverse samples taken in the 1980s and 1990s, and examined for internal consistency [Key et al., 2004], is compared to the modeled TA in the surface ocean calculated under constant scenario (Figure 3). The constant scenario is selected for this comparison because it assumes that the invasion of anthropogenic CO_2 does not lead to any shifts in calcification which would affect TA. In other model scenarios, calcification changes as a function of temporal evolution of the calcite saturation state.

[16] Global TA patterns in the modern ocean are well reproduced by the model. The maxima of surface TA are predicted and observed in the subtropical gyres at about 30°N and 30°S, most pronounced in the Atlantic Ocean, resembling the global salinity pattern. The values of TA decrease poleward with minimum values in the Arctic Ocean (not covered by the GLODAP data set) which is colder, fresher and thus less alkaline. An offshore gradient in the modeled TA values in the Arctic Ocean indicates the presence of river runoff.

4. Model-Data Comparison: Uncertainties and Natural Variability

[17] Model results are evaluated taking into account the natural variability in ocean carbonate chemistry. Data from the repeat hydrography program, as well as from the long-term time series stations were used to evaluate model results and to discern the typical amplitude of natural variability in CO_2-system parameters on decadal timescales.

[18] Repeat hydrographic transects of TA available through the Carbon Dioxide Information Analysis Center (CDIAC, http://cdiac.ornl.gov/) in the Atlantic, Pacific, and Indian Ocean are examined for possible trends and shifts in the surface and deep-ocean inventories. Changes in TA in the upper 100 m and below are calculated as the difference between the two years.

$$\Delta\text{Alk} = \text{Alk}_{latest} - \text{Alk}_{earliest} \qquad (3)$$

[19] We calculated ΔAlk on the basis of the repeat meridional transects in the Atlantic Ocean (A16S and A16N; see Figure 4), as well as in the Pacific Ocean transect (P15S) and the Indian Ocean transect (I03; see Figure 5). At a given location along the transect, the maximum calculated changes in TA between the two years, i.e., 2005 and 1991 (A16S), 2003 and 1993 (A16N), 2001 and 1996 (P15S) and 2003 and 1995 (I03) are up to ±34 μmol kg^{-1} (Table 1). This includes effects of seasonal, hydrographic and biological effects on TA, as well as methodological errors. However, the mean ΔAlk between the two years are only about 2 μmol kg^{-1} in the Atlantic Ocean transects and range from 5.7 to 9.3 in the Pacific Ocean and the Indian Ocean transects and thus indicate no detectable shift in the TA inventories that is significant over a time period of 14 years (see below).

[20] Changes in TA modeled under constant scenario for the upper 100 m and below are calculated as the difference between the two calculated TA fields averaged over the years corresponding to the repeat transects A16S, A16N (Figure 4), P15S and I03 (Figure 5) according to equation (3). Differences in modeled TA range from -0.4 to 0.4 μmol kg^{-1} with the mean difference being below 0.07 μmol kg^{-1} (Table 1). Small changes in modeled TA between different years are attributed to the nonlinearity of the biological processes despite the strictly recurrent ocean circulation used in model integrations (section 2.1). Overall, modeled TA tends to increase in the upper ocean by <0.1 μmol kg^{-1} in the equatorial Atlantic and Pacific Ocean and by about 0.1 in the Indian Ocean over the timescale of the observations (Figures 4 and 5). In deep waters, modeled changes in TA are about a factor of 4 smaller than in the upper 100 m.

[21] We have also compared calculated annual mean TA in the surface ocean layer to observations from the two deep ocean time series stations BATS (Bermuda Atlantic Time series Study) and ALOHA (A Long-Term Oligotrophic Habitat Assessment). BATS is located in the subtropical gyre of the NW Atlantic near Bermuda at 31° 43′N, 64° 10′W. Station ALOHA is located in the subtropical North Pacific Ocean near Hawaii at 22° 45′N, 158° 00′W. Both deep ocean stations are located beyond the coastal influence and
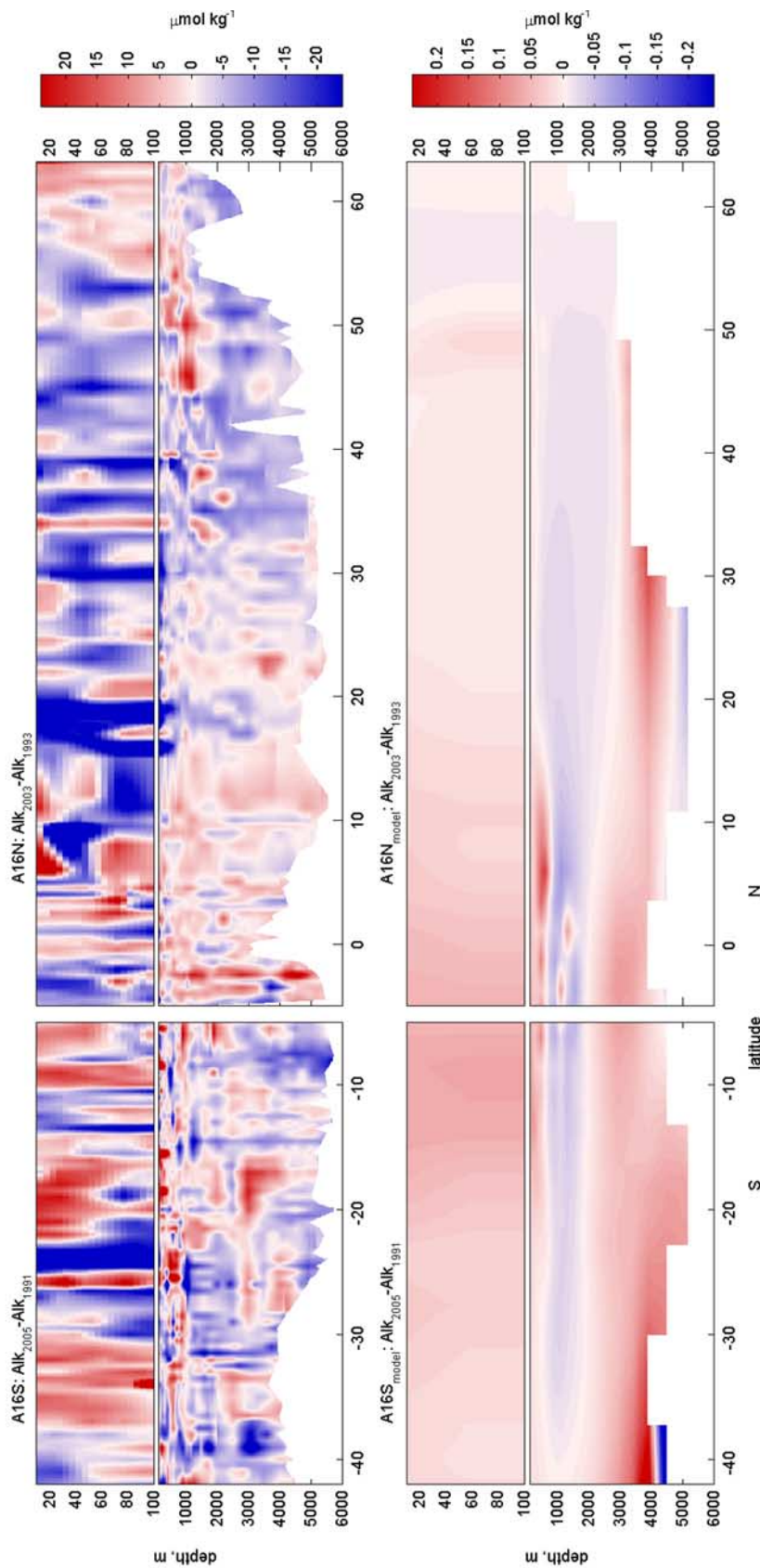
Figure 4. Changes in the total alkalinity (μmol kg^{-1}) in the Atlantic Ocean meridional transect calculated as the difference between years 2005 and 1991 for A16S (top left) and between 2003 and 1992 for A16N (top right) on the basis of repeat hydrographic section data in the upper 100 m and below and corresponding annual mean modeled changes calculated under constant scenario (bottom). Note the different scale bar units and color indexing of plots.
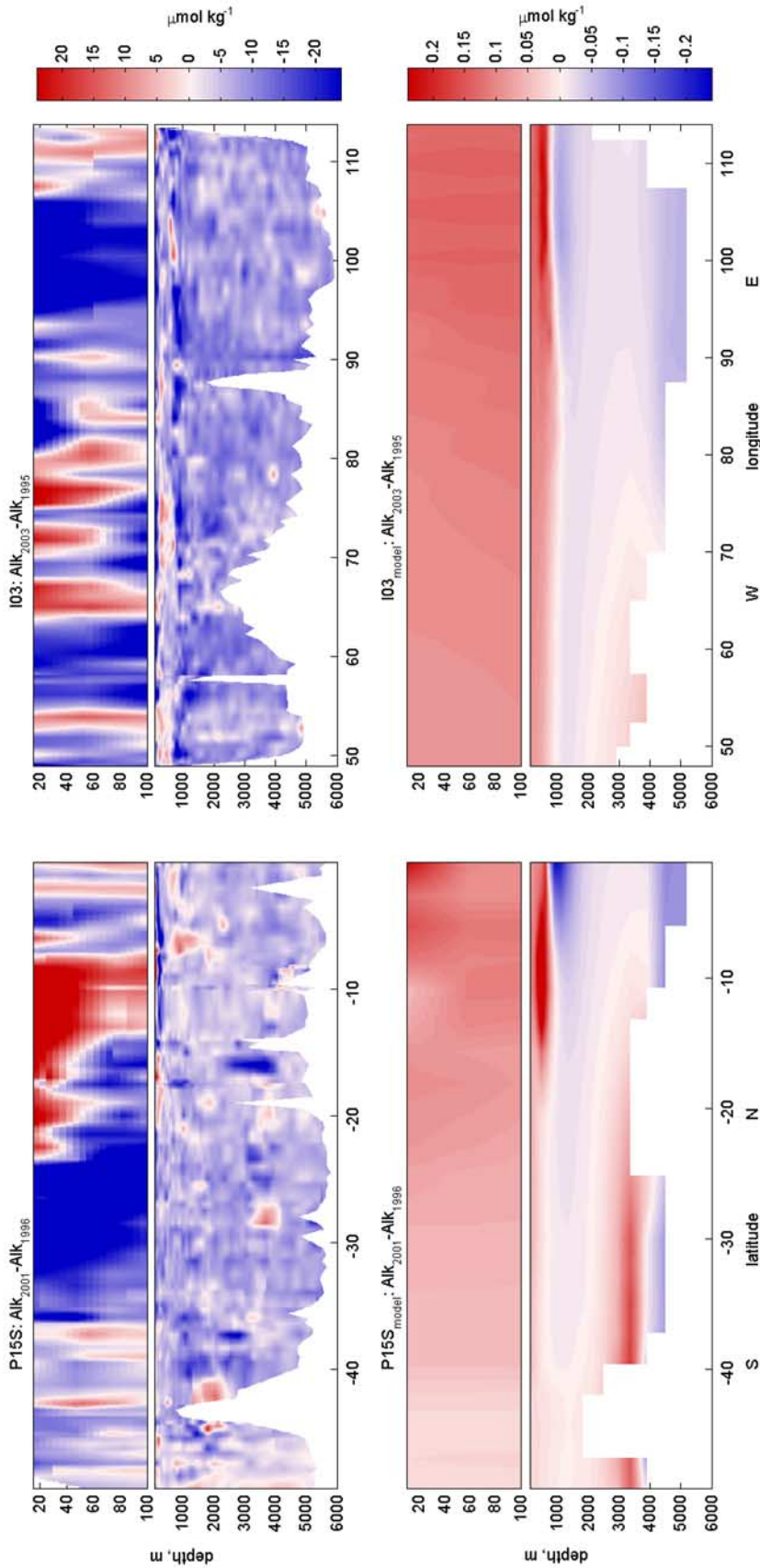
Figure 5. Changes in the total alkalinity (μmol kg^{-1}) in the Pacific Ocean meridional transect P15S (left) calculated as the difference between years 2001 and 1996 on the basis of repeat hydrographic section data in the upper 100 m and below and in the Indian Ocean zonal transect I03 calculated as the difference between years 2003 and 1995 (right) and corresponding annual mean modeled changes calculated under constant scenario (bottom). Note the different scale bar units and color indexing of plots.

Table 1. Mean and Range of Changes in the Total Alkalinity[a]

Transect	Years of Sampling	Observed ΔAlk, Upper 100 m: Mean and Range	Observed ΔAlk, Below: Mean and Range	Modeled ΔAlk, Upper 100 m: Mean and Range	Modeled ΔAlk, Below: Mean and Range
A16S	2005, 1995	−0.736 (−30.918−33.455)	−2.122 (−33.752−30.803)	0.040 (0.015−0.067)	0.016 (−0.380−0.320)
A16N	2003, 1993	−2.205 (−30.612−21.117)	−1.618 (−30.834−23.215)	0.012 (−0.011−0.059)	0.001 (−0.086−0.18)
P15S	2001, 1996	−6.168 (24.739−29.224)	−5.787 (−28.094−24.304)	0.073 (0.014−0.252)	0.025 (−0.229−0.374)
I03	2003, 1995	−9.372 (−28.819−29.425)	−8.511 (−31.285−15.860)	0.106 (0.085−0.138)	0.039 (−0.079−0.244)

[a]In the upper 100 m and below in the transects A16S, A16N, P15S, and I03 calculated as the difference between the two years of sampling (see equation (3)), on the basis of repeat hydrographic section data and on model calculations. Units are μmol kg^{-1}.

are representative for the open ocean. TA measured at BATS does not show any pronounced temporal trend in the period from 1988 to 2006 [*Bates*, 2007], absolute values ranged between 2385 and 2407 μmol kg^{-1} (Table 2). Similarly, TA at Station ALOHA measured during 1989–2006 does not exhibit a temporal trend, total values range from 2301 to 2324 μmol kg^{-1}. TA variability calculated by the model was <1 μmol kg^{-1} at both locations. Interannual mean modeled TA at BATS and ALOHA are 2378 and 2309 μmol kg^{-1}, respectively compared to the measured values of 2394 and 2311 μmol kg^{-1}. The correlation coefficient between measured and modeled TA time series for these two locations is 0.67 for BATS and 0.54 for ALOHA (Table 2) indicating positive tendency in the temporal variations of both measured and modeled TA for ALOHA and BATS time series.

[22] Trends in ocean chemistry caused by ocean acidification need to be separated from unrelated effects, such as changes in ocean circulation or shifts in remineralization rates [e.g., *Wanninkhof et al.*, 2006]. This allows identifying trends in the data due to ocean acidification, which will only become detectable when their effects are larger than the error bars of the measurements and when they exceed the natural variability of ocean carbonate chemistry. The mean ΔAlk for all analyzed vertical sections is <10 μmol kg^{-1}(Table 1). As an estimation of the decadal variability in the analyzed repeat transects and time series, we used the overall variability of the mean TA changes ($\sigma_{\Delta Alk}$) expressed by the standard deviation. This leads to the value $\sigma_{\Delta Alk}$ = ±9.8 μmol kg^{-1} used as a detection threshold indicative of the natural variability in the global TA distributions (this value is similar to those derived by *Lee et al.* [2006] and *Key et al.* [2004], on the basis of different approaches). For a given scenario, we are then able to predict at what point in time changes in surface calcification

lead to alterations of ocean chemistry that are detectable in the data and are statistically significant.

[23] Modeled TA in the Atlantic and Pacific oceans show no detectable temporal trend during the time period of comparison, which is in line with observations. This also holds for salinity-normalized TA observations, which we have tested, for example, for section A16N. A minor increase in the upper ocean over the last decades (Figures 4 and 5) remains within the range of natural variability (about ±10 μmol kg^{-1}) derived from mean decadal changes in observed TA.

5. Future Predictions

[24] In the following, we describe the model-predicted evolution of total alkalinity in the future as a function of different calcification scenarios. Temporal evolution of TA averaged over the Atlantic and Pacific Ocean during the simulation period is shown for all scenario runs (Figure 6). Calculated alkalinity increases throughout the simulation period in all scenarios. Declining saturation state for calcite (Figure 7) and shoaling of saturation horizons driven by the oceanic uptake of CO_2 result in (1) reduced $CaCO_3$ export fluxes in surface waters and (2) carbonate sediment dissolution in acidified water in the deep ocean due to exposure of sediments to undersaturated waters. Both processes increase the total alkalinity of seawater in the model.

[25] The calcite saturation state (Figure 7) and marine carbonate production decline until after the year 2100 when a peak in atmospheric CO_2 concentration of about 800 ppm is reached as a consequence of anthropogenic emissions (Figure 1). Although under the given emission scenario, calcification stops decreasing after 2100 in all calcification scenarios, total alkalinity continues to increase (Figure 6). TA in the model is sensitive to assumptions regarding initial

Table 2. List of Time Series Stations[a]

Data Set	Location	Years of Sampling	Measurements: TA Mean and Range (μmol/kg)	Model: TA Mean and Range (μmol/kg)	Correlation Coefficient[b]
BATS	31°40′N, 64°10′W	1988−2006	2393.76 (2384.93−2407.07)	2378.02 (2377.75−2378.33)	0.67
ALOHA	22°45′N, 158°00′W	1989−2006	2310.89 (2300.95−2323.73)	2308.73 (2308.56−2308.99)	0.54

[a]Used for the model evaluation, their geographical location, years of sampling, mean and range of measurements and modeled total alkalinity (TA) and correlation coefficients between measured and modeled TA.

[b]The correlation coefficient (R) between modeled and observed TA (TAm and TAo respectively) is given by $R = \sum_{i=1}^{n} (TA\mathrm{m}_i - \overline{TA\mathrm{m}}) (TA\mathrm{o}_i - \overline{TA\mathrm{o}}) \Big/ \sqrt{\sum_{i=1}^{n}(TA\mathrm{m}_i - \overline{TA\mathrm{m}})^2 \sum_{i=1}^{n}(TA\mathrm{o}_i - \overline{TA\mathrm{o}})^2}$.
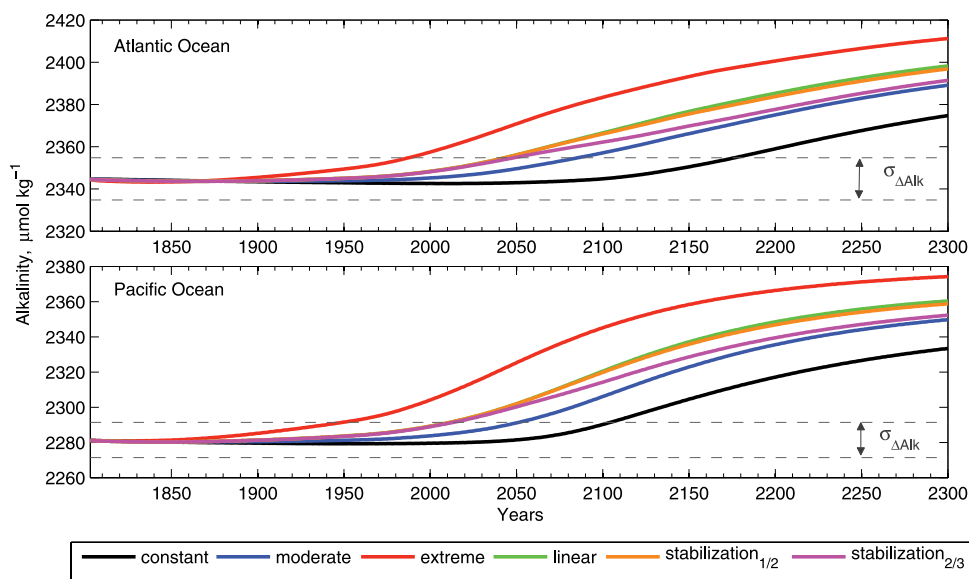
Figure 6. Temporal evolution of surface alkalinity (μmol kg^{-1}) calculated under different scenarios averaged over the Atlantic and Pacific oceans. Dashed lines show detection threshold value ($\sigma_{\Delta Alk}$ = ±9.8 μmol kg^{-1} with regard to preindustrial alkalinity) derived from mean decadal changes in observed total alkalinity (TA).

carbonate production rates. Because ocean circulation and biological parameters have no long-term trend in the model, the calculated changes in total surface alkalinity are due to changes in calcification and carbonate sediment dissolution. However, possible changes in surface CaCO$_3$ dissolution due to upwelling of more corrosive water along the continental shelf [*Feely et al.*, 2008] are not included in the model. As a result, the projected TA changes in the surface ocean are likely lower estimates.

[26] Given our model predictions based on different calcification scenarios, we predict that potential shifts in global TA inventories are currently not detectable in the ocean for all scenarios. Temporal evolution of alkalinity under all scenarios but the extreme one is identical until the end of 1990s (Figure 6). In the extreme scenario, alkalinity exhibits an increase already in the beginning of the 20th century. The detection threshold value for TA in the extreme scenario is exceeded around the 1990s in the Atlantic Ocean and in the year 1950 in the Pacific Ocean. If such large changes in the TA of about 40 μmol kg^{-1} in the Pacific Ocean (Figure 6) had occurred in the real ocean would they have been captured in observations? Unfortunately, reliable TA observations are available only since the 1980s and measurements of TA in the pre-industrial ocean do not exist. The changes in the TA predicted by the extreme scenario for the past two decades are about 7 μmol kg^{-1} in the Pacific Ocean and <2 μmol kg^{-1} in the Atlantic Ocean (Figure 6), falling within the range of natural variability. Therefore, it is
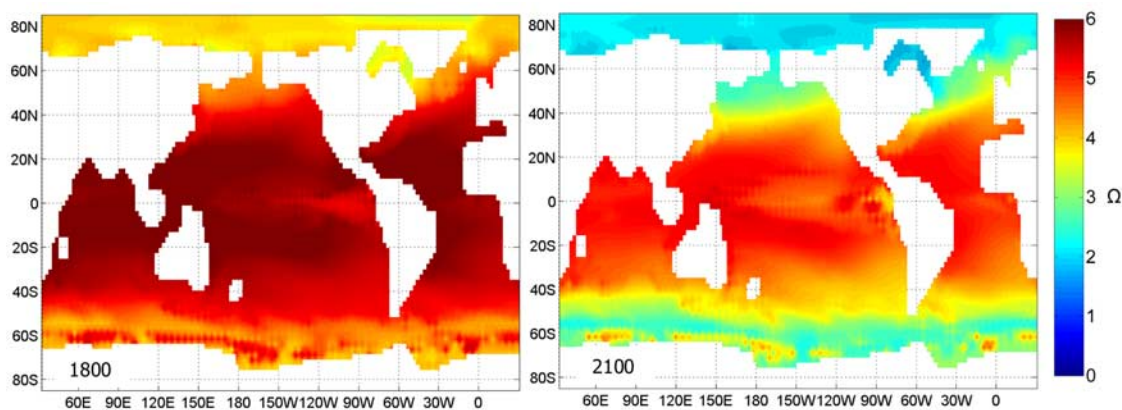
Figure 7. Saturation state of calcite (Ω) calculated under moderate scenario for the years (left) 1800 and (right) 2100.
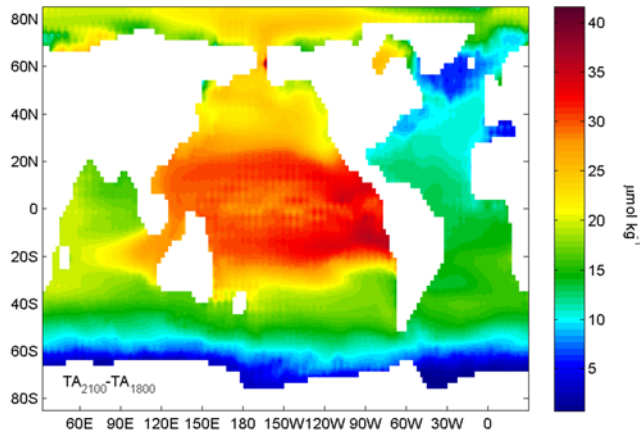
Figure 8. Differences in modeled surface alkalinity (μmol kg^{-1}) in the surface ocean between years 2100 and 1800 calculated under moderate scenario.

not possible to rule out this scenario on the basis of the current observations, although we consider it very unlikely. This scenario was designed upon calcification response in corals to decreasing saturation state reported from experimental studies (section 2.2) and may apply to local environments, e.g., where CaCO$_3$ production is dominated by corals.

[27] In the Pacific Ocean, spatially averaged TA overcomes the natural variability threshold exceeding the constant scenario by 10 μmol kg^{-1} already in year 2015 in linear and stabilization scenarios and around year 2050 in the moderate scenario. In the Atlantic Ocean, the threshold value (about 10 μmol kg^{-1}) is crossed around year 2035 in linear and stabilization scenarios and in year 2080 in the moderate one. In year 2100, the increase in TA for the linear scenario compared to the constant one reaches 20 μmol kg^{-1} in the Atlantic Ocean and 30 μmol kg^{-1} in the Pacific Ocean. Stabilization scenarios start to diverge from the linear one after 2040. According to model predictions, TA in different scenarios will increase by 50–80 μmol kg^{-1} compared to pre-industrial values by 2300.

[28] For the scenario when calcification rates stabilize after a reduction to 2/3 with respect to the pre-industrial saturation state (stabilization$_{2/3}$; see Figure 2), TA almost merges the moderate scenario by the end of the simulation period. The stabilization$_{1/2}$ scenario follows the linear one for the spatially averaged TA, indicating that a reduction > 50% in Ω occurs only locally in the linear scenario. Alkalinity in the constant scenario remains at the pre-industrial level until the end of the 21st century, increasing by 30 μmol kg^{-1} in year 2300. This increase is attributed to seafloor CaCO$_3$ dissolution (which will become increasingly important on longer timescales) and is consistent with our own predictions based on a simplified model that includes a sediment module [*Zeebe and Zachos*, 2007; *Zachos et al.*, 2008; *Zeebe et al.*, 2008].

[29] Model calculations suggest that the largest changes in surface TA due to changes in calcification in the future

(calculated as ΔAlk according to equation (3) for the years 2100 and 1800) will occur in the tropical and subtropical Pacific Ocean where TA in 2100 calculated under moderate scenario (Figure 8) may be 30–60 μmol kg^{-1} higher compared to the pre-industrial values (cf. Figure 3). The TA increase in the Arctic and the Indian Ocean is <30 μmol kg^{-1}, while in the Atlantic and Southern Ocean it is less than 25 μmol kg^{-1}. The TA increase predicted under the linear scenario is larger by about 10 μmol kg^{-1}.

[30] The calculated ratio in CaCO$_3$ production (P_{CaCO3}) in 2100 versus 1800 (Figure 9c) indicates that the relative decrease in high latitudes is stronger than in low latitudes because of lower initial CaCO$_3$ production and saturation state. The decrease in absolute rates of pelagic calcification is higher in the tropical waters in the areas of the greater extent of formation of CaCO$_3$ shells (Figure 9a). According to model calculations, the spatial distribution of pelagic CaCO$_3$ production calculated under the moderate scenario suggest that calcite production rates in the tropical and subtropical ocean with higher initial CaCO$_3$ production will drop by 20–50% in 2100 (Figure 9b).

6. Conclusions

[31] The model results show that alkalinity increases over time in all scenarios in which calcification decreases in response to changes in saturation state. This increase occurs because of decreased CaCO$_3$ export in surface waters and increased carbonate sediment dissolution at the seafloor. Given our model predictions based on different calcification scenarios, we conclude that potential changes in total alkalinity fields are not yet detectable in the global ocean.

[32] The extreme scenario suggests large shifts in the global TA already at present, which one would expect to be detectable in the observations. However, observations of the pre-industrial surface ocean TA do not exist and the time period of modern ocean TA observations is only two to three decades. As a result, TA changes modeled under the extreme scenario over the past two decades are still below the natural variability threshold. Thus, on the basis of the available observations, it is currently not possible to rule out the increase in the TA predicted by the extreme scenario. Although this scenario appears unlikely to be realized on the global scale, it could be occurring locally, for instance, in coastal environments where calcification is dominated by corals that are highly sensitive to changes in saturation state.

[33] The increase in alkalinity under moderate and linear scenarios exceeds the natural variability of about ±10 μmol kg^{-1} by the year 2040 and even earlier in the Pacific Ocean under the linear scenario. According to model predictions, TA will change slower in high latitudes than in the (sub)-tropics. However, relative changes in the calculated CaCO$_3$ production are stronger in polar regions. The model calculations indicate that the largest changes in the absolute values of surface alkalinity in the future will be expected in the subtropical Pacific and Atlantic oceans. In order to monitor and quantify such early signs of ocean acidification effects, we suggest to specifically target those regions during future ocean carbon programs.
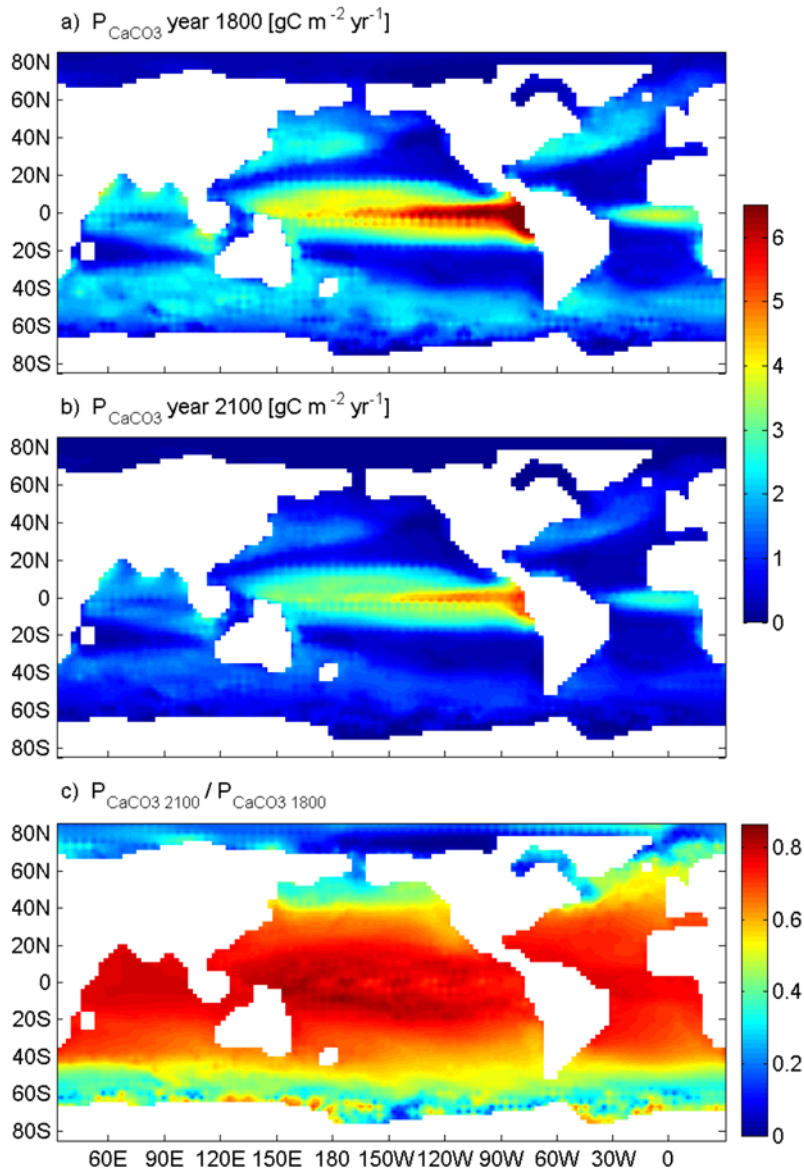
Figure 9. Pelagic $CaCO_3$ production (P_{CaCO3}, expressed in gC m^{-2} a^{-1}) calculated under moderate scenario for the years (a) 1800, (b) 2100, and (c) ratio of pelagic $CaCO_3$ production in years 2100 and 1800.

References

Andersson, A. J., F. T. Mackenzie, and A. Lerman (2006), Coastal, ocean CO_2-carbonic acid-carbonate sediment system of the Anthropocene, *Global Biogeochem. Cycles*, *20*, GB1S92, doi:10.1029/2005GB002506.

Archer, D., H. Kheshgi, and E. Maier-Reimer (1998), Dynamics of fossil fuel CO_2 neutralization by marine $CaCO_3$, *Global Biogeochem. Cycles*, *12*, 259–276, doi:10.1029/98GB00744.

Aumont, O., E. Maier-Reimer, S. Blain, and P. Monfray (2003), An ecosystem model of the global ocean including Fe, Si, P colimitations, *Global Biogeochem. Cycles*, *17*(2), 1060, doi:10.1029/2001GB001745.

Bates, N. R. (2007), Interannual variability of the oceanic CO_2 sink in the subtropical gyre of the North Atlantic Ocean over the last 2 decades, *J. Geophys. Res.*, *112*, C09013, doi:10.1029/2006JC003759.

Bijma, J., H. J. Spero, and D. W. Lea (1999), Reassessing foraminiferal stable isotope geochemistry: Impact of the oceanic carbonate system (experimental results), in *Use of Proxies in Paleoceanography: Examples From the South Atlantic*, edited by G. Fischer and G. Wefer, pp. 489–512, Springer, Berlin.

Caldeira, K., and M. E. Wickett (2003), Anthropogenic carbon and ocean pH, *Nature*, *425*, 365, doi:10.1038/425365a.

Dickson, A. G (1981), An exact definition of total alkalinity and a procedure for the estimation of alkalinity and total inorganic carbon from titration data, *Deep Sea Res., Part A*, *28*, 609–623, doi:10.1016/0198-0149(81)90121-7.

Feely, R. A., C. L. Sabine, J. M. Hernandez-Ayon, D. Ianson, and B. Hales (2008), Evidence for upwelling of corrosive "acidified" water onto the continental shelf, *Science*, *320*, 1490–1492, doi:10.1126/science.1155676.

Gazeau, F., C. Quiblier, J. M. Jansen, and J. P. Gatusso (2007), Impact of elevated CO₂ on shellfish calcification, *Geophys. Res. Lett.*, *34*, L07603, doi:10.1029/2006GL028554.

Gehlen, M., R. Gangsto, B. Schneider, L. Bopp, O. Aumont, and C. Ethe (2007), The fate of pelagic CaCO₃ production in a high CO₂ ocean: A model study, *Biogeosciences*, *4*, 505–519.

Heinze, C. (2004), Simulating oceanic CaCO₃ export production in the greenhouse, *Geophys. Res. Lett.*, *31*, L16308, doi:10.1029/2004GL020613.

Heinze, C., and E. Maier-Reimer (1999), *The Hamburg Oceanic Carbon Cycle Circulation Model Version "HAMOCC2s" for Long Time Integrations*, *Tech. Rep. 20*, 71 pp., Modellbetreuungsgruppe, Dtsch. Klimarechenzentrum, Hamburg, Germany.

Heinze, C., A. Hupe, E. Maier-Reimer, N. Dittert, and O. Ragueneau (2003), Sensitivity of the marine biospheric Si cycle for biogeochemical parameter variations, *Global Biogeochem. Cycles*, *17*(3), 1086, doi:10.1029/2002GB001943.

Intergovernmental Panel on Climate Change (2001), *Climate Change 2001: The Scientific Basis*, edited by J. T. Houghton et al., 881 pp., Cambridge Univ. Press, Cambridge, UK.

Intergovernmental Panel on Climate Change (2007), *Climate Change 2007: The Physical Science Basis*, edited by S. Solomon et al., 996 pp., Cambridge Univ. Press, Cambridge, UK.

Jones, J. B., E. H. Stanley, and P. J. Mulholland (2003), Increased alkalinity in the Mississippi, *Science*, *302*(5647), 985–987, doi:10.1126/science.302.5647.985c.

Key, R. M., A. Kozyr, C. L. Sabine, K. Lee, R. Wanninkhof, J. Bullister, R. A. Feely, F. Millero, C. Mordy, and T.-H. Peng (2004), A global ocean carbon climatology: Results from GLODAP, *Global Biogeochem. Cycles*, *18*, GB4031, doi:10.1029/2004GB002247.

Kleypas, J. A., R. W. Buddemeier, D. Archer, J.-P. Gattuso, C. Langdon, and B. N. Opdyke (1999), Geochemical consequences of increased atmospheric carbon dioxide on coral reefs, *Science*, *284*, 118–120, doi:10.1126/science.284.5411.118.

Kleypas, J. A., R. A. Feely, V. J. Fabry, C. Langdon, C. L. Sabine, and L. L. Robbins (2006), Impacts of ocean acidification on coral reefs and other marine calcifiers: A guide to future research, report of a workshop held 18–20 April 2005, St. Petersburg, Florida, sponsored by NSF, NOAA, and the U.S. Geological Survey, 88 pp.

Langdon, C., and M. J. Atkinson (2005), Effect of elevated pCO₂ on photosynthesis and calcification of corals and interactions with seasonal change in temperature/irradiance and nutrient enrichment, *J. Geophys. Res.*, *110*, C09S07, doi:10.1029/2004JC002576.

Langer, G., M. Geisen, K.-H. Baumann, J. Klaes, U. Riebesell, S. Thoms, and J. R. Young (2006), Species-specific responses of calcifying algae to changing seawater carbonate chemistry, *Geochem. Geophys. Geosyst.*, *7*, Q09006, doi:10.1029/2005GC001227.

Leclercq, N., J.-P. Gattuso, and J. Jaubert (2000), CO₂ partial pressure controls the calcification rate of a coral community, *Global Change Biol.*, *6*, 329–334, doi:10.1046/j.1365-2486.2000.00315.x.

Lee, K., et al. (2006), Global relationships of total alkalinity with salinity and temperature in surface waters of the world's oceans, *Geophys. Res. Lett.*, *33*, L19605, doi:10.1029/2006GL027207.

Maier-Reimer, E. (1993), Geochemical cycles in an ocean general circulation model: Preindustrial tracer distributions, *Global Biogeochem. Cycles*, *7*, 645–677, doi:10.1029/93GB01355.

Maier-Reimer, E., U. Mikolajewicz, and K. Hasselmann (1993), Mean circulation of the Hamburg LSG OGCM and its sensitivity to the thermohaline surface forcing, *J. Phys. Oceanogr.*, *23*, 731–757, doi:10.1175/1520-0485(1993)023<0731:MCOTHL>2.0.CO;2.

Nanninga, H. J., and T. Tyrrell (1996), Importance of light for the formation of algal blooms by Emiliania huxleyi, *Mar. Ecol. Prog. Ser.*, *136*, 195–203, doi:10.3354/meps136195.

Raven, J. A., K. Caldeira, H. Elderfield, O. Hoegh-Guldberg, P. Liss, U. Riebesell, J. Shepherd, C. Turley, and A. Watson (2005), Acidification due to increasing carbon dioxide, *Report 12/05*, 68 pp., Royal Soc., London.

Ridgwell, A. J., I. Zondervan, J. C. Hargreaves, J. Bijma, and T. M. Lenton (2007), Assessing the potential long-term increase of oceanic fossil fuel CO₂ uptake due to CO₂-calcification feedback, *Biogeosciences*, *4*, 481–492.

Riebesell, U., I. Zondervan, B. Rost, P. D. Tortell, R. E. Zeebe, and F. M. M. Morel (2000), Reduced calcification of marine plankton in response to increased atmospheric CO₂, *Nature*, *407*, 364–367, doi:10.1038/35030078.

Six, K. D., and E. Maier-Reimer (1996), Effects of plankton dynamics on seasonal carbon fluxes in an ocean general circulation model, *Global Biogeochem. Cycles*, *10*, 559–583, doi:10.1029/96GB02561.

Tyrrell, T., and A. Merico (2004), Emiliania huxleyi: Bloom observations and the conditions that induce them, in *Coccolithophores: From Molecular Processes to Global Impact*, edited by H. R. Thierstein and J. R. Young, pp. 75–97, Springer, Berlin.

Wanninkhof, R., S. Doney, J. L. Bullister, N. Gruber, C. Sabine, R. A. Feely, G. C. Johnson, and F. Millero (2006), Changes in inorganic carbon inventory in the Atlantic Ocean over the last decade, *Eos Trans. American Geophysical Union*, *87*(36), Ocean Sci. Meet. Suppl., Abstract OS52C-01.

Wolf-Gladrow, D. A., J. Bijma, and R. E. Zeebe (1999), Model simulation of the carbonate system in the microenvironment of symbiont bearing foraminifera, *Mar. Chem.*, *64*, 181–198, doi:10.1016/S0304-4203(98)00074-7.

Zachos, J. C., G. R. Dickens, and R. E. Zeebe (2008), An early Cenozoic perspective on greenhouse warming and carbon-cycle dynamics, *Nature*, *451*, 279–283, doi:0.1038/nature06588.

Zeebe, R. E., and D. A. Wolf-Gladrow (2001), *CO₂ in Seawater: Equilibrium, Kinetics, Isotopes*, Elsevier Oceanogr. Ser., vol. 65, 346 pp., Elsevier, Amsterdam.

Zeebe, R. E., and J. C. Zachos (2007), Reversed deep-sea carbonate ion basin-gradient during Paleocene-Eocene Thermal Maximum, *Paleoceanography*, *22*, PA3201, doi:10.1029/2006PA001395.

Zeebe, R. E., J. C. Zachos, K. Caldeira, and T. Tyrrell (2008), Oceans: Carbon emissions and acidification, *Science*, *321*, 51–52, doi:10.1126/science.1159124.

———————————

C. Heinze, Geophysical Institute and Bjerknes Centre for Climate Research, University of Bergen, Allegaten 70, 5007 Bergen, Norway. (christoph.heinze@gfi.uib.no)

T. Ilyina and R. E. Zeebe, Department of Oceanography, School of Ocean and Earth Science and Technology, University of Hawaii, 1000 Pope Road, Honolulu, HI 96822, USA. (ilyina@soest.hawaii.edu; zeebe@soest.hawaii.edu)

E. Maier-Reimer, Max Planck Institute for Meteorology, Bundesstrasse 53, 20146 Hamburg, Germany. (ernst.maier-reimer@zmaw.de)